# Si=X Multiple Bonding with Four-Coordinate Silicon? Insights into the Nature of the Si=O and Si=S Double Bonds in Stable Silanoic Esters and Related Thioesters: A Combined NMR Spectroscopic and Computational Study

Jan. D. Epping,[†] Shenglai Yao,[†] Miriam Karni,*,[‡] Yitzhak Apeloig,*,[‡] and Matthias Driess*,[†]

*Institute of Chemistry, Metalorganics and Inorganic Materials, Technische Universität Berlin, Strasse des 17. Juni 135, Sekr. C2, D-10623 Berlin, Germany and Schulich Faculty of Chemistry and the Lise Meitner-Minerva Center for Computational Quantum Chemistry, Technion - Israel Institute of Technology, Haifa 32000, Israel*

Received January 19, 2010; E-mail: matthias.driess@tu-berlin.de; chrmiri@tx.technion.ac.il; apeloig@technion.ac.il

***Abstract:*** The electronic structures and nature of silicon−chalcogen double bonds Si=X (X = O, S) with four-coordinate silicon in the unique silanoic silylester **2** and silanoic thioester **3** have been investigated for the first time, by $^{29}$Si solid state NMR measurements and detailed DFT and *ab initio* calculations. $^{29}$Si solid state NMR spectroscopy of the precursor silylene **1** was also carried out. The experimental and computational study of **2** and **3**, which was also supported by a detailed computational study of smaller model systems with Si=O and Si=S bonds, provides a deeper understanding of the isotropic and tensor components of their NMR chemical shifts. The general agreement between the experimental NMR spectra and the calculations strongly support our previous NMR assignment deduced from experiment. The calculations revealed that in **2** $\delta(^{29}\mathrm{Si}(=\mathrm{O}))_{\mathrm{iso}}$ is shifted upfield relative to $H_2Si=O$ by as much as 175 ppm; the substituents are responsible for ca. 100 ppm of this shift, while the remaining upfield shift is caused by change in the coordination number from three to four at the Si=O moiety. The change in coordination number leads to a nearly cylindrical symmetry in the plane which is perpendicular to the Si=O molecular axis ($\delta_{11} \approx \delta_{22}$), in contrast to the significant anisotropy found in this plane in typical doubly bonded compounds. The change in $r$(Si=O) or in the degree of pyramidality at the Si=O center which accompanies the change in coordination number has practically no effect on the chemical shift. $\delta(^{29}\mathrm{Si}(=\mathrm{S}))_{\mathrm{iso}}$ in **3** is shifted downfield significantly relative to that in **2**, and a similar trend is found in smaller models with Si=S vs those with Si=O subunits. This downfield shift can be explained by the smaller $\sigma-\pi^*$ energy difference in the Si=S bond, relative to that of the Si=O bond. The NMR measurements of **2** and **3** having a *four-coordinate* silicon−chalcogen moiety, and the calculations of their tensor components, their bond polarities, and their Wiberg bond indices revealed that the Si=X moieties in both **2** and **3** have a significant $\pi(\mathrm{Si}=\mathrm{X})$ character; yet, in both molecules there is a substantial contribution from a zwitterionic $\mathrm{Si}^+−\mathrm{X}^-$ resonance structure, which is more pronounced in **2**.

## 1. Introduction

The chemistry of stable main-group element compounds with silicon−heteroatom double bonds has witnessed tremendous progress over the past 25 years.[1−3] Presently, low-valent silicon compounds with multiple bonds to silicon and other main-group elements are no longer laboratory curiosities but indispensable building blocks in contemporary organosilicon chemistry and silicon-assisted organic synthesis due to the fact that Si=X compounds possess a unique reactivity. Since the seminal works by West et al. and Brook and co-workers who reported on the first isolable disilene (>Si=Si<)[4a] and silene (>Si=C<)[4b] in 1981, numerous isolable species with Si=X bonds with X being a group 13,[5] 14,[6−8] 15,[9−11] and 16 element[12−16] have been synthesized and characterized structurally. Isolable compounds

---

[†] Technische Universität Berlin.

[‡] Technion - Israel Institute of Technology.

(1) (a) Raabe, G.; Michl, J. In *The Chemistry of Organic Silicon Compounds*; Patai, S., Rappoport, Z., Eds.; Wiley: New York, 1989; Part 2, Chapter 17, pp 1015−1142. (b) Müller, T. Ziche, W.; Auner, N. In *The Chemistry of Organic Silicon Compounds*; Rappoport, Z., Apeloig, Y., Eds.; Wiley, Chichester, 1998; Vol. 2, part 2, pp 859−1062. (c) Tokitoh, N.; Okazaki, R. In *The Chemistry of Organic Silicon Compounds*; Rappoport, Z., Apeloig, Y., Eds.; Wiley: Chichester, 1998; Vol. 2, part 2, pp 1064−1103.

(2) *Advances in Organometallic Chemistry*; West, R., Stone, F. G. A., Eds.; Academic Press: San Diego, 1996; Vol. 39.

(3) Power, P. P. *Chem. Rev.* **1999**, *99*, 3463−3503.

(4) (a) West, R.; Fink, M. J.; Michl, J. *Science* **1981**, *214*, 1343−1344. (b) Brook, A. G.; Abdesaken, F.; Gutekunst, B.; Gutekunst, G.; Kallury, R. K. *J. Chem. Soc., Chem. Commun.* **1981**, 191−192.

(5) Nakata, N.; Sekiguchi, A. *J. Am. Chem. Soc.* **2006**, *128*, 422−423.

(6) West, R. *Polyhedron* **2002**, *21*, 467−472.

(7) Weidenbruch, M. *Organometallics* **2003**, *22*, 4348−4360.

(8) Tokitoh, N.; Okazaki, R. *Adv. Organomet. Chem.* **2001**, *47*, 121−166.

(9) Driess, M. *Adv. Organomet. Chem.* **1996**, *39*, 193−229.

with a silicon−silicon triple bond have also been reported recently.[17−19]

However, stable silicon homologues of ubiquitous ketones ($R_2Si=O$) and carboxylic acids ($RSi(=O)OH$) remained elusive for a long time. This is mainly due to the challenging task of preventing the highly polarized $Si=O$ double bond from oligomerization, which proceeds with no barrier,[20−22] in contrast to their carbon analogues or any other related silicon−heteroatom $\pi$-system. Additionally, silanoic acids ($RSi(=O)OH$; with R = H, alkyl) tend to isomerize to their divalent silicon tautomers ($RO(OH)Si:$, silylenes).[23] Therefore, silanones[24,25] and silanoic acid derivatives[23,25,26] are elusive species which have predominantly been investigated in cryogenic argon matrices. However, inspired by the work of Corriu and co-workers, who reported the first silanethione ($Si=S$) and silaneselone ($Si=Se$) derivatives supported by an intramolecular N→Si donor−acceptor bond,[12] some of us were able to synthesize isolable compounds with $Si=O$ double bonds. This has been achieved by conversion of the recently synthesized stable zwitterionic silylene **1**[27] (Scheme 1) in the presence of water and water−borane adducts to give the corresponding siloxysilylene (Scheme 2, **a**) precursor and silaformamide−borane (Scheme 2, **b**) complexes,[28] respectively. Furthermore, the first isolable silanoic silylester[29] **2** (Scheme 1) was subsequently prepared by facile monooxygenation of the aforementioned siloxysilylene with $N_2O$.[29] In a similar fashion, the corresponding thio-, (**3**) seleno-, and telluroesters[30a] were synthesized from the same siloxysilylene

**Scheme 1.** Stable Silylene **1**, Silanoic Silylester **2**, and Silanoic Thioester **3** (R = 2,6-*i*Pr$_2$C$_6$H$_3$)
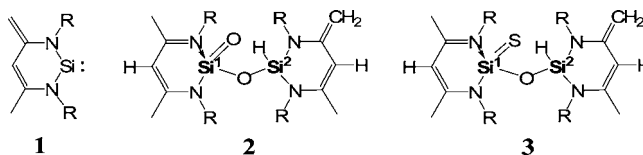


**Scheme 2.** Siloxysilylene (a) and Silaformamide-Borane (b)
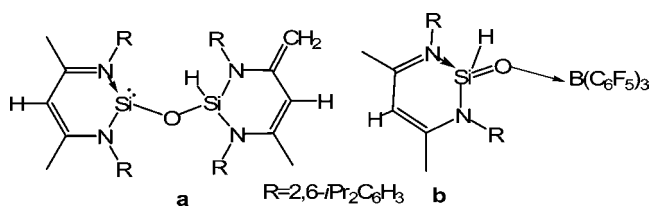


precursor by oxidation with the respective elemental chalcogens. Recently, West et al. reported on another type of isolable $Si=Se$ compounds with donor-supported $Si=Se$ $\pi$-bonds.[30b] Likewise, inspired by the work of Robinson and co-workers[31] who described an isolable N-heterocyclic carbene (NHC) supported disilicon compound L→:Si=Si:←L (with L = NHC) with silicon in the formal oxidation state zero, Driess et al. succeeded in the synthesis of a NHC-supported stable silanone by oxidation of an NHC−silylene adduct with $N_2O$,[32,33b] as well as the NHC-supported chalcogenone analogues for S, Se, and Te.[33]

The isolable silicon−chalcogen doubly bonded compounds mentioned above represent donor-coordinated Si=X systems with betaine-like resonance structures. However, apart from applying a somewhat plausible Lewis structure formalism for their description, the knowledge of the electronic nature of donor-stabilized Si=X systems is scarce. To model and to understand the nature and electronic structure of such donor-stabilized silicon−chalcogen doubly bonded systems in more detail, we performed NMR spectroscopic measurements and theoretical calculations. Solid-state NMR is a very powerful tool for obtaining structural and electronic information for organic molecules like carbenes.[34] In contrast to solution NMR, solid-state NMR measurements allow for the extraction of anisotropic (direction-dependent) chemical shielding information that is averaged in solution by fast Brownian motion. Thus, solid-state NMR spectroscopy provides a superb probe of the electronic environment of NMR-active nuclei and yields insights into the dependence of particular shielding or deshielding influences on the electronic and geometric structure of the molecules.[35] Components of the chemical shift tensor can be extracted in a straightforward manner from static NMR powder spectra or by

(10) Driess, M.; Block, S.; Brym, M.; Gamer, M. T. *Angew. Chem., Int. Ed.* **2006**, *45*, 2293–2296.

(11) Hemme, I.; Klingebiel, U. *Adv. Organomet. Chem.* **1996**, *39*, 159–192.

(12) Arya, R.; Boyer, J.; Carré, F.; Corriu, R.; Lanneau, G.; Lappasset, J.; Perrot, M.; Priou, C. *Angew. Chem., Int. Ed. Engl.* **1989**, *28*, 1016–1018.

(13) Suzuki, H.; Tokitoh, N.; Okazaki, R. *J. Am. Chem. Soc.* **1994**, *116*, 11578–11579.

(14) Suzuki, H.; Tokitoh, N.; Okazaki, R.; Nagase, S.; Goto, M. *J. Am. Chem. Soc.* **1998**, *120*, 11096–11105.

(15) Okazaki, R.; Tokitoh, N. *Acc. Chem. Res.* **2000**, *33*, 625–630.

(16) Iwamoto, T.; Sato, K.; Ishida, S.; Kabuto, C.; Kira, M. *J. Am. Chem. Soc.* **2006**, *128*, 16914–16920.

(17) Wiberg, N.; Vasisht, K. S.; Fischer, G.; Meyer, P. *Z. Anorg. Allg. Chem.* **2004**, *630*, 1823–1828.

(18) Sekiguchi, A.; Kinjyo, R.; Ichinohe, M. *Science* **2004**, *305*, 1755–1757.

(19) Sasamori, T.; Hironaka, K.; Sugiyama, Y.; Takagi, N.; Nagase, S.; Hosoi, Y.; Furukawa, Y.; Tokitoh, N. *J. Am. Chem. Soc.* **2008**, *130*, 13856–13857.

(20) Apeloig, Y. Theoretical aspects of organosilicon compounds. In *The Chemistry of Organic Silicon Compounds*; Patai, S., Rappoport, Z., Eds.; Wiley: New York, 1989; Vol. 1, Chapter 2, p 57 and references cited therein.

(21) Kapp, J.; Remko, M.; Schleyer, P. v. R. *J. Am. Chem. Soc.* **1996**, *118*, 5745–5751.

(22) Kimura, M.; Nagase, S. *Chem. Lett.* **2001**, 1098–1099.

(23) Becerra, R.; Bowes, S.-J.; Ogden, J. S.; Cannady, J. P.; Adamovic, I.; Gordon, M. S.; Almond, M. J.; Walsh, R. *Phys. Chem. Chem. Phys.* **2005**, *7*, 2900. and cited references therein.

(24) Khabashesku, V. N.; Kerzina, Z. A.; Kudin, K. N.; Nefedov, O. M. *J. Organomet. Chem.* **1998**, *566*, 45–59.

(25) Maier, G.; Meudt, A.; Jung, J.; Pacl, H. Matrix isolation studies of silicon compounds. In *The Chemistry of Organic Silicon Compounds*; Patai, S., Rappoport, Z., Eds.; Wiley: New York, 1998; Vol. 2, Chapter 2, p 1143 and references cited therein.

(26) Patyk, A.; Sander, W.; Gauss, J.; Cremer, D. *Angew. Chem., Int. Ed. Engl.* **1989**, *28*, 898–900.

(27) (a) Driess, M.; Yao, S.; Brym, M.; van Wüllen, C.; Lentz, D. *J. Am. Chem. Soc.* **2006**, *128*, 9628–9629. (b) Xiong, Y.; Yao, S.; Driess, M. *Chem.-Asian J.* **2009**, *4*, 1323–1328.

(28) Yao, S.; Brym, M.; van Wüllen, C.; Driess, M. *Angew. Chem., Int. Ed.* **2007**, *46*, 4159–4162.

(29) Yao, S.; Xiong, Y.; Brym, M.; Driess, M. *J. Am. Chem. Soc.* **2007**, *129*, 7268–7269.

(30) (a) Yao, S.; Xiong, Y.; Brym, M.; Driess, M. *Chem. Asian J.* **2008**, *3*, 113–118. (b) Mitra, A.; Wojcik, J. P.; Lecoanet, D.; Muller, T.; West, R. *Angew. Chem., Int. Ed.* **2009**, *48*, 4069–4072.

(31) (a) Wang, Y.; Xie, Y.; Wei, Y.; King, R. B.; Schaefer, H. F., III; Schleyer, P. v. R.; Robinson, G. H. *Science* **2008**, *321*, 1069–1071. (b) Wang, Y.; Quillian, B.; Wei, P.; Xie, Y.; Wannere, C. S.; King, R. B.; Schaefer, H. F., III; von R. Schleyer, P.; Robinson, G. H. *J. Am. Chem. Soc.* **2008**, *130*, 3298–3299. (c) Wang, Y.; Xie, Y.; Wei, P.; King, R. B.; Schaefer, H. F., III; von R. Schleyer, P.; Robinson, G. H. *J. Am. Chem. Soc.* **2008**, *130*, 14970–14971.

(32) Xiong, Y.; Yao, S.; Driess, M. *J. Am. Chem. Soc.* **2009**, *131*, 7562–7563.

(33) (a) Xiong, Y.; Yao, S.; Driess, M. *Chem.−Eur. J.* **2009**, *15*, 8542–8547. (b) Yao, S.; Xiong, Y.; Driess, M. *Chem.−Eur. J.* **2010**, *16*, 1281–1288.

(34) Arduengo, A. J.; Dixon, D. A.; Kumashiro, K. K.; Lee, C.; Power, W. P.; Zilm, K. W. *J. Am. Chem. Soc.* **1994**, *116*, 6361–6167.

a Hertzfeld−Berger analysis of sideband intensities in MAS (magic angle spinning) NMR spectra at slow spinning frequencies.[36] In recent years ^{29}Si solid-state NMR measurements have been instrumental in gaining insight into the electronic environments of silicon nuclei in disilenes,[37a] silenes,[37b] disilynes,[38,39] and silylenes[40,41] Results from NMR measurements yield particularly valuable information when correlated with those obtained by calculations of the chemical shift tensors of model systems. Theoretical model calculations allow for detailed insights into the electronic nature of the silicon environments in the compounds also via the calculation of e.g. bond orders or partial charges. Good agreement between theoretical and experimental [29]Si chemical shift data validates the accuracy of the computational model which is used, provides insights into the electronic structure of the molecules studied, and supports the chemical shift assignments deduced from experiment.

In this work, we present a detailed study on the electronic structure of the donor-coordinated silicon−chalcogen $\pi$-systems in the silanoic silylester **2** and the corresponding silanoic thioester **3** as well as on the electronic nature of the stable silylene precursor **1**. We present the results of ^{29}Si solid-state NMR measurements of the three compounds and their chemical shift tensor components. To allow interpretation of these data, we carried out DFT and *ab initio* quantum mechanical calculations on several model systems for both the silanoic silylester **2** and the silanoic thioester **3**. Overall, the studies clearly show that the silicon−chalcogen bonds have considerable double bond character, despite the fact that silicon is four-coordinated.

## 2. Experimental Section

**2.1. Sample Preparation.** The stable silylene **1**, the silanoic silylester **2**, and the silanoic thioester **3** were synthesized according to the published procedures.[27,29,30]

**2.2. NMR Measurements.** Solid state [29]Si{[1]H} static and MAS cross-polarization (CP)[42,43] measurements were carried out on a Bruker Avance II spectrometer at an external magnetic field of 9.4 T (i.e., a ^{1}H resonance frequency of 400 MHz) using a standard Bruker 4 mm double-resonance H-X MAS probe. The CP spectra were recorded with a cross-polarization time of 2 ms, and composite pulse ^{1}H decoupling was applied during the acquisition. Between 3500 (12 kHz MAS) and 16 000 transients were recorded with a relaxation delay of 2 s. The spectra were referenced externally to TMS (tetramethylsilane) using TKS (*tetrakis*(trimethylsilyl)silane) as a secondary reference. The isotropic chemical shifts were verified by measurements at multiple MAS rotation frequencies.

**2.3. Computational Methods.** The computational study was performed using Density Functional Theory (DFT)[44] and *ab initio* quantum mechanical computational methods. Geometries were fully

optimized using the hybrid density functional method B3LYP[45] with the 6-31G(d),[46] 6-311G(d,p),[47] 6-311+G(d,p),[48] and cc-PVTZ[49] basis sets. The smaller molecules were optimized also using the *ab initio* MP2[50] level of theory with a variety of basis sets as indicated in the discussion. Frequencies were calculated for all model systems to identify them as minima.

The NMR chemical shielding $\sigma$ were calculated using the GIAO method[51] with the B3LYP hybrid functional.[52] For several smaller models we also used the MP2[50] and CCSD[53] *ab initio* methods with the 6-311G(3d) and cc-PVTZ basis sets. The chemical shift values $\delta$ are calculated relative to the calculated values of the isotropic chemical shielding of tetramethylsilane (TMS): $\delta = \sigma_{TMS} - \sigma$, where $\sigma_{TMS}$ is the calculated value at a particular level (Table 1S in Supporting Information).

The Natural Bond Orbital program (NBO 5.0)[54] was used to calculate atomic charges as well as bond orders and to perform Natural Chemical Shift analysis (NCS).[55]

All calculations were performed using the Gaussian 03[56] series of programs. The CCSD NMR chemical shifts were calculated using ACESII.[57]

## 3. Results and Discussion

**3.1. Experimental Results.** The N-heterocyclic silylene **1** shows a unique reactivity toward electrophiles and nucleophiles attributed to its ylide-like resonance structure with positive charge accumulation at the cyclic $C_3N_2Si$ backbone, high electrophilicity at the silicon(II) center,[27] and high nucleophilicity at the exocyclic vinylic carbon. Thus, **1** reacts as a betaine

(35) (a) Grant, D. M. In *Encyclopedia of NMR Spectroscopy*; Grant, D. M., Webb, G. A., Eds.; Wiley: New York, 1996; p 4316. (b) Facelli, J. C.; Grant, D. M.; Michl, J. *Acc. Chem. Res.* **1987**, *20*, 152–158.
(36) Herzfeld, J.; Berger, A. E. *J. Chem. Phys.* **1980**, *73*, 6021–6030.
(37) (a) West, R.; Cavalieri, J.; Buffy, J. J.; Fry, C.; Zilm, K. W.; Duchamp, J.; Kira, M.; Iwamoto, T.; Mueller, T.; Apeloig, Y. *J. Am. Chem. Soc.* **1997**, *19*, 4972–4976. (b) Buffy, J. J.; West, R.; Bendikov, M.; Apeloig, Y. *J. Am. Chem. Soc.* **2001**, *123*, 978–979.
(38) Kravchenko, V.; Kinjo, R.; Sekiguchi, A.; Ichinohe, M.; West, R.; Balazs, Y. S.; Schmidt, A.; Karni, M.; Apeloig, Y. *J. Am. Chem. Soc.* **2006**, *128*, 14472–14473.
(39) Karni, M.; Apeloig, Y.; Tagaki, N.; Nagase, N. *Organometallics* **2005**, *24*, 6319–6330.
(40) West, R.; Buffy, J. J.; Haaf, M.; Müller, T.; Gehrhus, B.; Lappert, M. F.; Apeloig, Y. *J. Am. Chem. Soc.* **1998**, *120*, 1639–1640.
(41) Müller, T. *J. Organomet. Chem.* **2003**, *686*, 251–256.
(42) Pines, A.; Gibby, M. G.; Waugh, J. S. *J. Chem. Phys.* **1973**, *59*, 569–590.
(43) Taylor, R. E. *Concepts Magn. Reson., Part A* **2004**, *22A* (1), 37–49.
(44) (a) Koch, W.; Holthausen, M. C. *A Chemist's Guide to Density Functional Theory*; Wiley-VCH, 2000. (b) Parr, R. G.; Yang, W. *Density-Functional Theory of Atoms and Molecules*; Oxford University Press: New York, 1989.
(45) (a) Becke, A. D. *J. Chem. Phys.* **1993**, *98*, 5648–5652. (b) Lee, C.; Yang, W.; Parr, R. G. *Phys. Rev. B* **1988**, *37*, 785–789. (c) Vosko, S. H.; Wilk, L.; Nusair, M. *Can. J. Phys.* **1980**, *58*, 1200–1211.
(46) (a) First row elements: Hehre, W. J.; Ditchfield, R.; Pople, J. A. *J. Chem. Phys.* **1972**, *56*, 2257. Hariharan, P. C.; Pople, J. A. *Theoret. Chimica Acta* **1973**, *28*, 213–222. (b) Second row elements: Francl, M. M.; Petro, W. J.; Hehre, W. J.; Binkley, J. S.; Gordon, M. S.; DeFrees, D. J.; Pople, J. A. *J. Chem. Phys.* **1982**, *77*, 3654–3655.
(47) (a) For first row elements: Krishnan, R.; Binkley, J. S.; Seeger, R.; Pople, J. A. *J. Chem. Phys.* **1980**, *72*, 650–654. (b) For second row elements: McLean, A. D.; Chandler, G. S. *J. Chem. Phys.* **1980**, *72*, 5639–5648.
(48) Diffuse exponents: Clark, T.; Chandrasekhar, J.; Spitznagel, G. W.; Schleyer, P. v. R. *J. Comput. Chem.* **1983**, *4*, 294–301.
(49) (a) Woon, D. E.; Dunning, T. H., Jr. *J. Chem. Phys.* **1993**, *98*, 1358–1371. (b) Dunning, T. H., Jr. *J. Chem. Phys.* **1989**, *90*, 1007–1023.
(50) (a) Møller, C.; Plesset, M. S. *Phys. Rev.* **1934**, *46*, 618–622. (b) Pople, J. A.; Binkley, J. S.; Seeger, R. *Int. J. Quantum Chem.* **1976**, *10*, 1–19.
(51) (a) London, F. *J. Phys. Radium* **1937**, *8*, 397–409. (b) Ditchfield, R. *Mol. Phys.* **1974**, *27*, 789–807. (c) Wolinski, K.; Hinton, J. F.; Pulay, P. *J. Am. Chem. Soc.* **1990**, *112*, 8251–8260.
(52) (a) For some of the model systems we have used the HCTH407[52b] general gradient approximation (GGA) functional, the results are almost identical to those calculated using B3LYP and are thus not shown. . (b) Boese, A. D.; Handy, N. C. *J. Chem. Phys.* **2001**, *114*, 5497–5503.
(53) (a) Cizek, J. *Adv. Chem. Phys.* **1969**, *14*, 35. (b) Purvis, G. D.; Bartlett, R. J. *J. Chem. Phys.* **1982**, *76*, 1910–1918. (c) Scuseria, G. E.; Janssen, C. L.; Schaefer, H. F., III. *J. Chem. Phys.* **1988**, *89*, 7382–7387. (d) Scuseria, G. E.; Schaefer, H. F., III. *J. Chem. Phys.* **1989**, *90*, 3700–3703. (e) Gauss, J.; Stanton, J. F. *J. Chem. Phys.* **1995**, *102*, 251–253. (f) Gauss, J.; Stanton, J. F. *J. Chem. Phys.* **1995**, *103*, 3561–3577.
(54) Glendening, E. D.; Reed, A. E.; Carpenter, J. E.; Weinhold, F. *NBO*, version 5.0.
(55) Bohmann, J. A.; Farrar, T. C.; Weinhold, F. *J. Chem. Phys.* **1997**, *107*, 1173–1184.
(56) Frisch, M. J. *Gaussian 03*, revision D.02; Gaussian, Inc.: Wallingford, CT, 2004.
(57) Stanton, J. F.; Gauss, J.; Watts, J. D.; Szalay, P. G.; Bartlett, R. J. *ACES II*, Mainz-Austin-Budapest version 2005
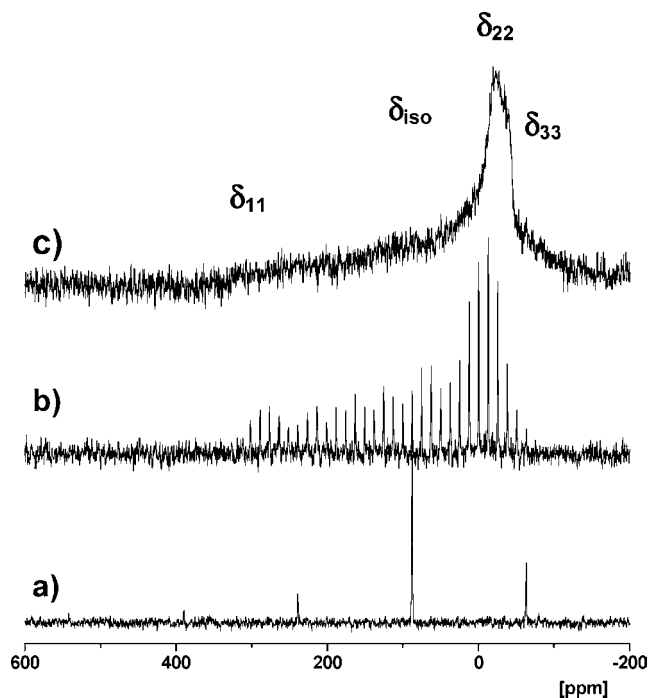
**Figure 1.** Solid-state $^{29}$Si {$^1$H}CP NMR spectra of the silylene **1** under (a) MAS conditions with a spinning frequency of 12 kHz, (b) MAS conditions with a spinning frequency of 1 kHz, (c) static conditions.

**Table 1.** Experimental Parameters of the $^{29}$Si Chemical Shift Tensor obtained from Solid-State $^{29}$Si NMR Measurements of **1**, **2**, and **3** [in ppm]

| Compound | $\delta_{iso}$ | $\delta_{11}$ | $\delta_{22}$ | $\delta_{33}$ | $\Delta\delta^a$ | $\delta_{iso}$ | $\delta_{11}$ | $\delta_{22}$ | $\delta_{33}$ | $\Delta\delta^b$ |
|---|---|---|---|---|---|---|---|---|---|---|
| **1** | 88 | 320 | −15 | −63 | 383 | | | | | |
| | | Si=O | | | | | Si−O | | | |
| **2** | −85 | −10 | −30 | −200 | 190 | −56 | −20 | −60 | −95 | 75 |
| | | Si=S | | | | | Si−O | | | |
| **3** | −38.7 | 87 | 11 | −215 | 302 | −53.5 | −3 | −54 | −104 | 101 |

$^a$ CSA = −216, −180, and −275 ppm in **1**, **2**, and **3** respectively.
$^b$ CSA = −55 and −76 ppm in **2** and **3**, respectively.

molecule with electrophiles of the type R−X (R = H, silyl; X = halogen, triflate) to give 1,4-adducts as kinetic products which subsequently isomerize to the corresponding 1,1-adducts.[27] Remarkably, the reactivity of **1** is different from that of its germanium homologue toward R−X electrophiles which leads exclusively to 1,4 adducts.[58] The higher stability of the 1,4 adducts in the case of germanium can be rationalized by the larger inert-pair effect for Ge(II) vs Si(II).[59]

To study the nature of the electronic structure of silylene **1** in more detail, DFT and Nuclear Independent Chemical Shift (NICS) calculations as well as solution-state $^1$H, $^{13}$C, and $^{29}$Si NMR have been carried out before,[27] but $^{29}$Si chemical shift anisotropy (CSA) parameters from solid-state NMR measurements are presented here for the first time. Figure 1a displays the $^{29}$Si{$^1$H} CP MAS NMR spectrum of silylene **1** recorded at a MAS frequency of 12 kHz. The spectrum exhibits a single sharp resonance at $\delta$ = 88 ppm which is accompanied by spinning sidebands distanced 12 kHz from the resonance. This isotropic $^{29}$Si chemical shift is identical to the corresponding $^{29}$Si chemical shift observed in solutions ($\delta$ = 88.4 ppm).[27a] The comparison shows that the isotropic $^{29}$Si chemical shift of **1** is predominately determined by the electronic structure of a distinct silylene molecule since there are no visible intermolecular effects on the $^{29}$Si chemical shift. It also shows that no significant conformational changes occur in solution relative to the solid state. The chemical shift of 88 ppm suggests a similar electronic situation as observed in other N-heterocyclic, p$_\pi$−p$_\pi$-conjugated silylenes.[40,60]

Figure 1b and 1c display the $^{29}$Si{$^1$H} CP NMR spectra of silylene **1** at 1 kHz MAS rotation and under static conditions,

(58) Driess, M.; Yao, S.; Brym, C.; van Wüllen, C. *Angew. Chem., Int. Ed.* **2006**, *45*, 4349–4352.
(59) Becerra, R.; Boganov, S. E.; Egorov, M. P.; Faustov, V. I.; Nefedov, O. N.; Walsh, R. *J. Am. Chem. Soc.* **1998**, *120*, 12657–12665.

respectively. It is clearly visible that at spinning speeds as low as 1 kHz the envelope of the spinning sideband pattern corresponds to the static powder pattern revealing the CSA that is averaged by fast MAS. The chemical shift tensor components which are listed in Table 1 were determined from these spectra.

As reported for other N-heterocyclic silylenes,[40,41] silylene **1** shows a strongly deshielded $\delta_{11}$ component of the chemical shift tensor resulting in a highly anisotropic chemical shift tensor with a span ($\Delta\delta$) of 383 ppm and a CSA[61] of −216 ppm. In silylenes, the deshielded component $\delta_{11}$ is usually oriented perpendicular to the molecular axis and lies in the plane of the divalent silicon and its two substituent atoms.[41] As commonly observed for silylenes, this tensor component is also in silylene **1**, by far the largest, and therefore determines mostly the isotropic $^{29}$Si NMR chemical shift. In contrast, the tensor components $\delta_{22}$ and $\delta_{33}$ have similar magnitudes and are in the expected chemical shift range for sp$^3$-silicon atoms. These findings are similar to those of other N-heterocyclic p$_\pi$−p$_\pi$ donor−acceptor stabilized silylenes.

Silanoic silylester **2** shows a significant upfield shift in the solution $^{29}$Si NMR spectrum relative to silylene **1**. The NMR of **2** displays two sets of resonances for the two chemically inequivalent $^{29}$Si nuclei at $\delta$ = −55.0, −55.5 ppm (each a doublet, attributed to the siloxy group, $^1J_{Si,H}$ = 281 Hz) and −85.1, −85.8 ppm (each a singlet, attributed to L′Si(=O)).[29] The appearance of two closely spaced resonances at both $\delta$ = −55 ppm and −85 ppm reveals the presence of mixtures of two rotational isomers in different ratios. The two isomers result from the presence of a tetracoordinate stereogenic silicon atom and hindered rotation around the Si−O bond of the Si−O−Si moiety. Remarkably, $\delta(^{29}$Si) in the L′Si=O moiety in **2** is shifted to a higher field than that observed for the silaformamide−borane complex LSi(H)=O→B(C$_6$F$_5$)$_3$ (Scheme 2, **b**; $\delta$ = −61.5 ppm).[28] Although to a lesser extent than in the silaformamide−borane complex, this indicates some degree of Si=O $\pi$-bonding interaction in **2** in spite of the presence of a tetracoordinate silicon (see discussion below). It is interesting to note that the chemical shift of the tetravalent sp$^3$ Si$^2$ atom in the siloxy moiety of $\delta$ = −56 ppm is at a significantly lower field (more deshielded) compared to the chemical shift of the Si$^1$ atom in the L′Si=O moiety of $\delta$ = −88 ppm, in contrast to the common expectation for chemical shifts of sp$^2$ vs sp$^3$ hybridized atoms.[62] What is the electronic nature of the Si=O bond? What causes the significant upfield shift of its $\delta(^{29}$Si)? To answer these questions, and to obtain a more profound insight into the electronic structure of compound **2**, we studied the silanoic

(60) Denk, M.; Lennon, R.; Hayashi, R.; West, R.; Belyakov, A. V.; Verne, H. P.; Haaland, A.; Wagner, M.; Metzler, N. *J. Am. Chem. Soc.* **1994**, *116*, 2691–2692.
(61) CSA = $\delta_{33}$−($\delta_{11}$ + $\delta_{22}$)/2 or CSA = $\sigma_{33}$−($\sigma_{22}$ + $\sigma_{11}$)/2); with $\delta_{33}$ and $\sigma_{33}$ representing the highest field tensor components. The span $\Delta\delta$ = |$\delta_{33}$−$\delta_{11}$|.
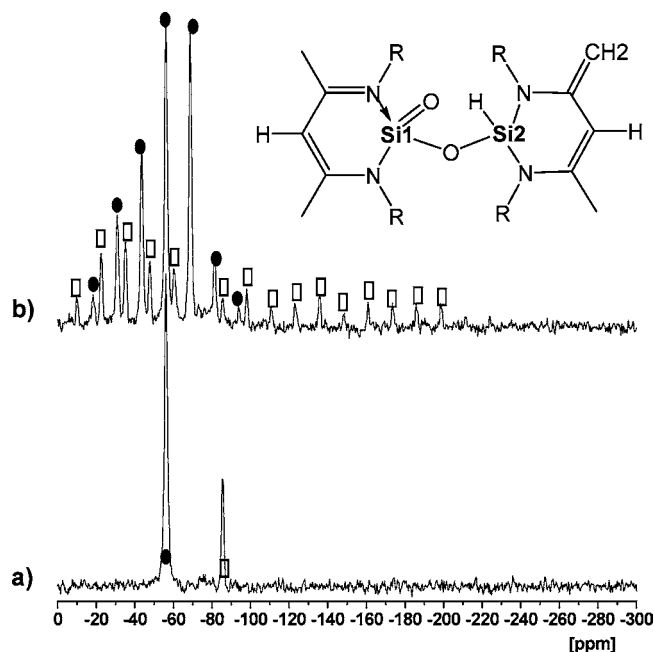
**Figure 2.** Solid-state $^{29}$Si {$^1$H}CP NMR spectra of the silanoic silylester **2** under MAS conditions with a spinning frequency of (a) 12 kHz and (b) 1 kHz. Resonances and spinning sidebands corresponding to Si$^1$ and Si$^2$ are marked with open squares and filled circles, respectively.

silylester **2** by $^{29}$Si solid state NMR and accompanied it by a detailed computational study.

Figure 2a shows the $^{29}$Si{$^1$H} CP MAS NMR spectrum of silanoic silylester **2** recorded at a MAS frequency of 12 kHz. The spectrum exhibits two sharp resonances at $\delta = -56$ and $-86$ ppm. These shifts correspond well to those measured in solution indicating no visible intermolecular or conformational effects on the $^{29}$Si chemical shifts. Figure 2b displays the $^{29}$Si{$^1$H} CP MAS NMR spectrum of **2** at 1 kHz MAS rotation.

Chemical shift tensor components extracted from this spectrum are listed in Table 1. The resonance corresponding to the siloxy group generates few spinning sidebands, indicating a narrow static $^{29}$Si powder pattern with a small span of $\Delta\delta = 75$ ppm and CSA of $-55$ ppm. Also, the chemical shift tensor components $\delta_{11} - \delta_{33}$ are in the expected chemical shift range for sp$^3$-silicon atoms, indicating a relatively isotropic chemical shift tensor typical of tetravalent $^{29}$Si atoms in N-sila-heterocycles.[41] The resonance corresponding to the L′Si=O moiety shows a very different behavior. A multitude of spinning sidebands reflects a broad NMR powder pattern with a broad span of $\Delta\delta = 190$ ppm and a large CSA of $-180$ ppm, a chemical shift anisotropy that is nearly as large as that for the divalent silylene **1**. It has been shown before that in many cases large CSA values indicate the presence of $\pi$-bonds.[63,64] Measured CSA values of compounds with C=Si,[37b] Si=Si,[37a,65,66]

(62) $\delta(^{29}$Si) in H$_3$C—SiH$_3$ and H$_2$C=SiH$_2$ are−70.0 and +62.6 ppm, respectively (B3LYP/6-311G(3d)); $\delta(^{13}$C) in H$_3$C—CH$_3$ and H$_2$C=CH$_2$ are 6.5 and 123.5 ppm, respectively (exp.); $\delta(^{29}$Si) of Si2 and Si1 in H$_3$CSi1(=O)O—Si$^2$H$_3$ (**6—O**) are−44.7 and 20.0 ppm, respectively (B3LYP/6-311G(3d), Table 2).
(63) Zilm, K. W.; Conlin, R. T.; Grant, D. M.; Michl, J. *J. Am. Chem. Soc.* **1980**, *102*, 6672–6676.
(64) Beeler, A. J.; Orendt, A. M.; Grant, D. M.; Cutts, P. W.; Michl, J.; Zilm, K. W.; Downing, J. W.; Facelli, J. C.; Schindlet, M. S.; Kutzelnigg, W. *J. Am. Chem. Soc.* **1984**, *106*, 7672–7676.
(65) Auer, D.; Strohmann, C.; Arbuznikov, A. V.; Kaupp, M. *Organometallics* **2003**, *22*, 2442–2449.
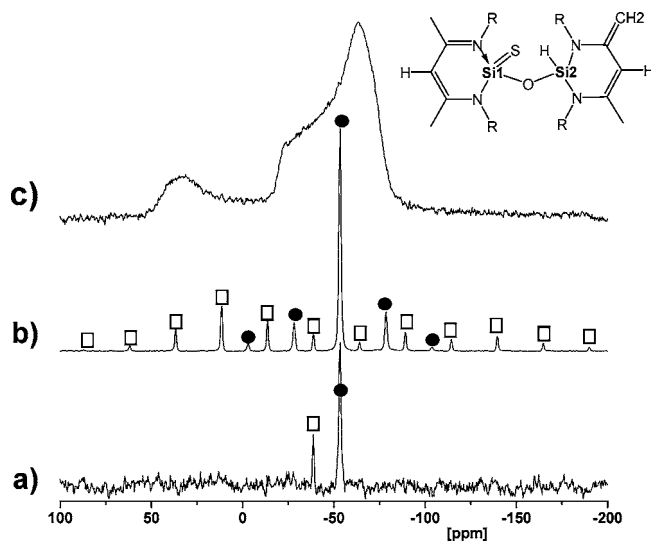(66) Auer, D.; Kaupp, M.; Strohmann, C. *Organometallics* **2005**, *24*, 6331.



**Figure 3.** Solid-state $^{29}$Si {$^1$H}CP NMR spectra of the silanoic thioester **3** under (a) MAS conditions with a spinning frequency of 12 kHz, (b) MAS conditions with a spinning frequency of 1 kHz, and (c) static conditions. Resonances and spinning sidebands corresponding to Si1 and Si2 are marked with open squares and filled circles, respectively.

and Sn=Sn[67] bonds revealed large CSA values, consistent with the existence of the proposed $\pi$-bonds. It should be noted though that the absolute size of the CSA (or span $\Delta\delta$) value does not reflect the $\pi$-bond strength, especially in comparing CSA values for different nuclei (see Figure 5).

The solution $^{29}$Si NMR spectrum of the silanoic thioester **3** shows a similar pattern to that of silanoic silylester **2**. The $^{29}$Si NMR spectrum shows two sets of resonances for the two chemically nonequivalent $^{29}$Si nuclei at $\delta = -53.5$ ppm (doublet, attributed to the siloxy group, $^1J_{Si,H} = 286$ Hz) and at $-40.7$, $-41.3$ ppm (each a singlet, attributed to L′Si=S).[27] The chemical shift of the $^{29}$Si nucleus in the L′Si=S moiety is shifted somewhat downfield relative to that of the Si atom in the siloxy moiety, and it is shifted significantly downfield relative to that of the Si atom in the L′Si=O moiety in silanoic silylester **2**. These comparisons may reflect the existence of a Si=S $\pi$-bond character in spite of the tetracoordinate-pyramidal structure of the Si$^1$ atom. To improve our understanding of the electronic structure and nature of bonding in L′Si=S, we have also studied the silanoic thioester **3** by $^{29}$Si solid state NMR accompanied by a computational analysis.

Figure 3a shows the $^{29}$Si{$^1$H} CP MAS NMR spectrum of silanoic thioester **3** recorded at a MAS frequency of 12 kHz. The spectrum exhibits two sharp resonances at $\delta -54$ and $-39$ ppm. These shifts correspond well to those measured in solution indicating marginal, if any, intermolecular or conformational effects on the $^{29}$Si chemical shifts. Figure 3b and 3c display the $^{29}$Si{$^1$H} CP NMR spectra of the silanoic thioester **3** at 1 kHz MAS rotation and under static conditions, respectively. Chemical shift tensor components extracted from these spectra are listed in Table 1. The static spectrum in Figure 3c nicely traces out the, partly overlapping, powder patterns of the two distinct isotropic resonances that could be identified under fast MAS conditions. In the spectrum recorded under slow MAS at 1 kHz spinning frequency (Figure 3b) it becomes more evident that the resonance corresponding to the siloxy group generates few

(67) Zilm, K. W.; Lawless, G. A.; Merrill, R. M.; Millar, J. M.; Webb, G. G. *J. Am. Chem. Soc.* **1987**, *109*, 7236–7238.

spinning sidebands, indicating a narrow static $^{29}$Si powder pattern with a relatively narrow span of $\Delta\delta = 101$ ppm and CSA of $-76$ ppm. Similar to the silanoic silylester **2**, the chemical shift tensor components $\delta_{11} - \delta_{33}$ are in the expected chemical shift range for sp$^3$-silicon atoms, indicating a relatively isotropic chemical shift tensor typical of tetravalent $^{29}$Si atoms in N-heterocycles.

Overall, the siloxy group in silanonic thioester **3** shows a somewhat increased chemical shift anisotropy relative to the corresponding silanoic ester **2**, reflecting the influence of the larger but less electronegative sulfur atom. Again, the resonance corresponding to the L′Si=S moiety shows a very different behavior. A multitude of spinning sidebands reflects a broad NMR powder pattern with a wide span of $\Delta\delta = 300$ ppm and a large CSA of $-275$ ppm, both being larger than that observed for the silanoic ester **2**.[68] This large anisotropy may suggest the presence of a Si=S $\pi$-bond character in **3**. Note that the larger CSA in **3** compared with **2** is not a definite indication that the $\pi$-bond character in **3** is larger than that in **2**.

**3.2. Computational Results.** To gain further insight into the electronic structure of the silicon-chalcogen double bonds in silanoic ester **2** and silanoic thioester **3**, we performed *ab initio* and DFT calculations of the chemical shift tensor components for **2** and **3** and for a set of model molecules containing Si=O and Si=S bonds which are used for the evaluation of the effect of substituents and of coordination on the structures, chemical shifts, bond polarities, and bond orders.

**3.2.1. Stuctures, NMR Analysis, and Bond Properties of Silanoic Ester 2 and Si=O Containing Model Systems.** Schematic structures and calculated optimized bond lengths of **2** and of 14 model molecules with Si=O bonds are shown in Figure 4. The experimental bond lengths extracted from the X-ray structure of **2**[29] are listed in bold letters below the values of the calculated geometry. The calculated values of the $^{29}$Si chemical shift tensor components $\delta_{11} - \delta_{33}$ and their span $\Delta\delta$ of **2** and of the model molecules are presented in Table 2

**3.2.1.1. Structures.** In **4-O**−**10-O** and in **14-O** the Si(=O) center is tricoordinate and has a planar structure, while in **11-O**, **12-O**, **13-O**, and **2** it is tetracoordinate and has a nonplanar structure.

The calculated Si=O bond length in H$_2$Si=O is 1.528, 1.535, and 1.523 Å at B3LYP, MP2, and CCSD, respectively, (using 6-311G(d,p) basis set; 1.537 Å at B3LYP/TZVP).[28] The gas-phase Si=O bond length measured by rotational submillimeter-wave spectra is $1.515 \pm 0.002$ Å.[69a] Thus, relative to the B3LYP bond length, $r$(Si=O) is elongated with MP2 and shortened with CCSD but it is still by 0.008 Å longer than the experimental one.[69b] Nevertheless, our goal is to calculate the geometry and NMR chemical shifts of **2** and **3**; we will mostly use geometries calculated at the B3LYP/6-31G(d) or B3LYP/6-311G(d,p) level of computation as the *ab initio* correlated methods with larger basis sets are prohibitive.

Substituents, i.e., hydroxy, silyloxy, or an amino group, have a marginal effect on the Si=O bond length and it lies in the range of 1.523−1.530 Å in **5-O**−**10-O**. In silaformamide **11-**

**O**, the Si=O bond is stabilized by complexation with two neighboring nitrogens and the two Si−N distances are the same. The silicon center is *tetracoordinate and pyramidal* ($\Sigma\alpha_i = 328$, Scheme 3), and as a result the Si=O bond is lengthened to 1.544 Å (B3LYP/6-31G(d), 1.553 Å at B3LYP/TZVP[28]). It also exhibits relatively long Si−N bonds of 1.831 Å (X-ray Si−N bond lengths in the silaformamide−borane complex (Scheme 2b) are 1.781 and 1.783 Å)[28] compared to those in **6-O**−**10-O** and to $r$(Si−N) = 1.729 (B3LYP/6-311G(d,p)) in H$_3$Si−NH$_2$.

A similar degree of pyramidality and Si−N bond lengthening is also found in silanoic silylester **12-O**, in **13-O**, and in the experimental silanoic silylester **2**. When one of the complexing amino groups is rotated away from the Si=O bond (**14-O**) and cannot interact with the silanone center, the Si=O bond length is similar to that in **4-O**−**10-O**. The ammonia−silacarbamate complex **15-O** is a simple model for complexes **12-O**, **13-O**, and **2**; it shows a slightly elongated Si=O bond and a relatively long H$_3$N−Si bond of 1.980 Å. Complexation stabilizes the silacarbamate−ammonia complex **15-O** by 24.9 kcal/mol (B3LYP/6-311G(d,p)) relative to NH$_3$ and H$_2$NSi(=O)OSiH$_3$.[70]

The calculated structure of **2** deviates somewhat from the X-ray structure. The main deviation is in a shorter calculated Si=O bond (1.542 Å (calc.) vs 1.579 Å (exp.)) and longer Si−N bonds (1.865 Å and 1.842 Å (calc.) vs 1.783 Å and 1.768 Å (exp.)). This is not a result of the relatively simple calculation method (B3LYP/6-31G(d)), since the calculations of H$_2$Si=O show that actually the B3LYP/6-31G(d) calculation leads to a slightly elongated Si=O bond, both relative to the experimental value and relative to CCSD calculations with larger basis sets (Figure 4). One may argue that B3LYP is not an adequate method for calculating complexation, but we find that the Si=O bond calculated for **12-O** at MP2/6-31G(d) is actually even slightly shorter than the B3LYP one. These and other discrepancies between the calculated and experimental structure (Figure 4) may result from a shallow potential surface with many local minima for **2**. In addition, a statistical disorder in the position of the Si=O moiety has been observed in the X-ray structure with a population ratio of 0.67/0.33 which may lead to the longer bond measured experimentally.

We also note that, in contrast to **2**, an excellent agreement in the Si=S bond length is found between the calculated (B3LYP/6-31G(d)) and the disorder-free X-ray structure of the analogous silanoic thioester **3** (Figure 7).

**3.2.1.2. $^{29}$Si NMR Chemical Shifts.** $^{29}$Si isotropic chemical shifts and their tensor components were calculated at the B3LYP/6-211G(3d) level (unless stated otherwise) and are shown in Table 2. For representative model compounds **7-O** (Table 2S in the Supporting Information) and **8-O** (Table 2), we have also repeated the NMR calculations at MP2 and CCSD with the 6-311G(3d) basis set and with the larger cc-PVTZ basis set. There is an overall downfield shift in $\delta(^{29}$Si=O)$_{iso}$ of 22 and 20.4 ppm in **7-O** and **8-O**, respectively, upon changing the level of calculation from B3LYP/6-311G(3d) to CCSD/cc-PVTZ, and only 3.8 and 5.3 ppm, respectively, on going from B3LYP/cc-PVTZ to CCSD/cc-PVTZ. We have therefore concluded that the B3LYP/cc-PVTZ level is appropriate for calculating the NMR chemical shifts of the larger systems, including that of **2**. Downfield shifts of ca. 17 ppm are calculated for **12-O** and **13-O** and of ca. 15 ppm are calculated for **2** (in

(68) The CSA of $^{29}$Si is larger when the silicon atom is bonded to a second row atom, e.g., in H$_2$C=SiH$_2$ and in H$_2$Si=SiH$_2$ the calculated (at B3LYP/6-311G(3d)//B3LYP/6-311G(3d)) $^{29}$Si CSA is −193.1 and −217.3 ppm, respectively, reflecting a downfield shift of the $\delta_{11}$ tensor component in the latter ($\delta_{11} = 272.3$ and 286.5 ppm, respectively).

(69) (a) Bogey, M.; Delcroix, B.; Walters, A.; Guillemin, J.-C. *J. Mol. Spectrosc.* **1996**, *175*, 421. (b) 1.514 Å using the CCSD(T) method with the Martin−Taylor core correlated basis set: Martin, J. M. L. *J. Phys. Chem. A* **1998**, *102*, 1394.

(70) Calculated by the following formula: $E$[H$_2$N(NH$_3$)Si(=O)OH, $r$(Si−NH$_3$) = 6.0 Å]− $E$[H$_2$N(NH$_3$)Si(=O)OH, $r$(Si−NH$_3$) = 1.980 Å]. $\Delta E$(**14-O**− **13-O**) = 52.7 kcal/mol (at B3LYP/6-31G(d)).
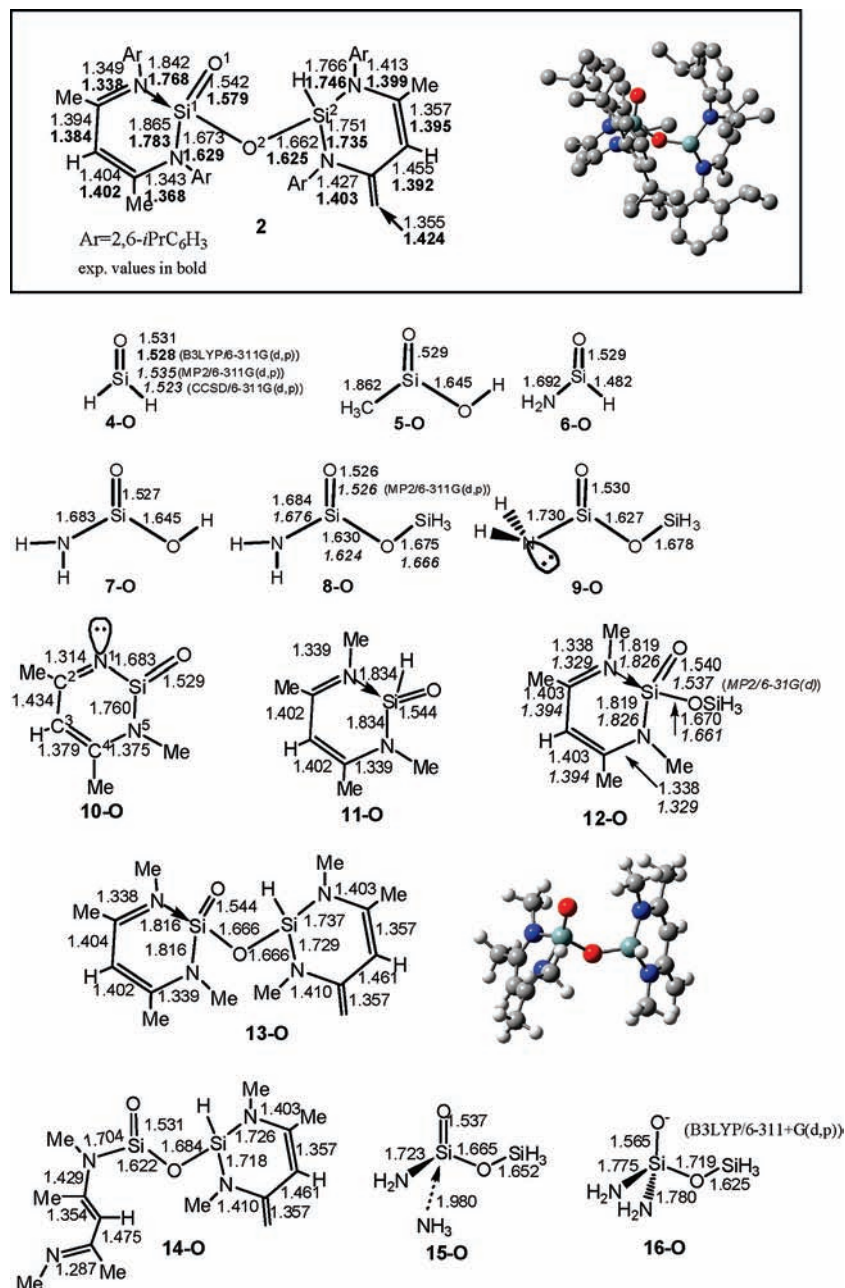
**Figure 4.** Optimized structures (at BLYP/6-31G(d), unless stated otherwise) of silanoic silylester **2** and of model compounds **4-O** to **16-O** containing Si=O bonds. Bond lengths are given in Å. In the ball and stick models, red balls = O, blue balls = N, green-gray balls = Si, and gray balls = C. The hydrogens in the ball and stick model of **2** are omitted for clarity.

both optimized and experimental geometries) upon going from B3LYP/6-311G(3d) to B3LYP/cc-PVTZ, a change which improves significantly the agreement between the calculated and experimental values of $\delta(^{29}\text{Si})_{\text{iso}}$ in **2**. The changes in the chemical shifts of Si−(O) in **8-O**, **12-O**, **13-O**, and **2** caused by changing the computational method are small.

Table 2 shows that $\delta(^{29}\text{Si})_{\text{iso}}$ values of **2** (at B3LYP/cc-PVTZ using both the optimized and X-ray structures) match the experimental NMR data very well with a deviation of less than 6 ppm. Slightly larger deviations are found for the individual tensor components, and the agreement is better when the X-ray geometry is used for the calculations, with a maximal deviation of 14 ppm for $\delta_{33}$. When the calculated geometry is used the deviation in $\delta_{33}$ increases to ca. 50 ppm, but the deviation of $\delta_{11}$ and $\delta_{22}$ is small. The overall good agreement between

experiment and theory for **2** indicates the high reliability of the computed isotropic chemical shift and tensor values as well as the reliability of the experimental X-ray and NMR measurements.

The results presented in Table 2 show that $\delta(^{29}\text{Si}(=O))_{\text{iso}}$ in **2** is shifted **upfield** by as much as **175 ppm** relative to $\delta(^{29}\text{Si}(=O))_{\text{iso}}$ in **4-O,** the prototype of a Si=O double bond. What causes this large shift? Substituent effects? Structural effects? Coordination to Si? How does the orientation and the size of the chemical shift tensor components change from the prototypical trigonal $H_2Si=O$ to the tetracoordinate $Si^1=O^1$ bond in **2**? What conclusions can be drawn from the analysis of the NMR spectrum regarding the nature of the $Si^1=O^1$ bond in **2**? To answer these questions we will analyze and discuss the isotropic chemical shift and the anisotropic chemical shift tensors

***Table 2.*** Calculated $^{29}$Si NMR Chemical Shifts$^a$ of Silanoic Silylester **2** and of Model Molecules with a Si=O Bond$^b$

| compound | Si=O | | | | | Si–O | | | | |
|---|---|---|---|---|---|---|---|---|---|---|
| | $\delta_{iso}$ | $\delta_{11}$ | $\delta_{22}$ | $\delta_{33}$ | $\Delta\delta$ | $\delta_{iso}$ | $\delta_{11}$ | $\delta_{22}$ | $\delta_{33}$ | $\Delta\delta$ |
| **4-O** | 72.2 | 318.7 | 8.6 | −110.7 | 429.4 | – | – | – | – | – |
| **5-O** | 25 (32.0)$^c$ | 193.3 (228.2)$^c$ | 58.7 (58.2)$^c$ | −177 (−190.5)$^c$ | 370.3 (418.7)$^c$ | – | – | – | – | – |
| **6-O** | 12.6 | 201.6 | 15.8 | −179.6 | 381.2 | | | | | |
| **7-O** | −17.8 | 113.8 | 32.3 | −199.5 | 313.3 | – | – | – | – | – |
| **8-O** | | | | | | | | | | |
| B3LYP/6-311G(3d) | −28.9 | 107.9 | 25.2 | −219.9 | 327.8 | −42.8 | −5.1 | −8.2 | −115.0 | 109.9 |
| MP2/6-311G(3d) | −23.8 | 102.7 | 33.6 | −207.8 | 310.5 | −42.2 | −2.6 | −5.9 | −118.2 | 115.6 |
| CCSD/6-311G(3d) | −20.7 | 103.6 | 37.1 | −202.8 | 306.4 | −37.4 | 1.6 | −1.0 | −112.7 | 114.3 |
| B3LYP/cc-PVTZ | −13.8 | 128.7 | 34.0 | −204.2 | 332.9 | −36.5 | 4.5 | −1.5 | −112.4 | 116.9 |
| MP2/cc-PVTZ | −12.0 | 115.2 | 42.6 | −193.9 | 309.1 | −39.0 | −3.5 | −6.5 | −107.0 | 103.5 |
| CCSD/cc-PVTZ | −8.5 | 116.1 | 47.3 | −188.8 | 304.9 | −35.5 | −2.4 | −5.0 | −99.1 | 96.7 |
| **9-O** | −8.7 | 142.6 | 47.8 | −216.5 | 359.1 | −41.7 | −3.6 | −8 | −216.5 | 109.9 |
| **10-O** | −8.5 | 165.1 | 30.2 | −220.9 | 386.0 | – | – | – | – | – |
| **11-O**$^d$ | −82.1 | 28.4 | −16.4 | −258.4 | 286.8 | – | – | – | – | – |
| **12-O**$^d$ | | | | | | | | | | |
| B3LYP/6-311G(3d) | −91.3 | −6.5 | −8.1 | −259.2 | 252.7 | −55.1 | −13.0 | −19.9 | −132.3 | 119.3 |
| B3LYP/cc-PVTZ | −73.7 | 9.4 | 9.2 | −239.7 | 249.1 | −44.8 | 1.0 | −8.1 | −127.3 | 128.3 |
| **13-O** | | | | | | | | | | |
| B3LYP/6-311G(3d) | −89.7 | −6.5 | −13.1 | −249.5 | 243.0 | −62.3 | −23.9 | −75.7 | −87.3 | 63.4 |
| B3LYP/cc-PVTZ | −72.3 | 9.2 | 3.6 | −229.6 | 238.8 | −46.6 | −7.3 | −62.0 | −70.5 | 63.2 |
| **14-O** | −35.9 | 83.4 | 23.1 | −214.2 | 297.6 | −57.2 | −18.2 | −63.9 | −89.6 | 71.4 |
| **15-O** | −79.8 | 17.3 | −7.5 | −249.3 | 266.6 | −54.5 | −14.1 | −19.2 | −130.1 | 116.0 |
| **16-O**$^e$ | −71.9 | −3.6 | −19.7 | −192.6 | 189 | −73.2 | −23.5 | −29.7 | −166.2 | 142.7 |
| **2** (opt. geom.) | | | | | | | | | | |
| B3LYP/6311G(3d) | −102.8 | −14.8 | −31.3 | −262.1 | 247.2 | −66.3 | −29.0 | −73.0 | −96.5 | 67.5 |
| B3LYP/cc-PVTZ | −88.1 | 0.0 | −16.4 | −248.0 | 248.0 | −53.5 | −12.1 | −59.7 | −88.6 | 76.5 |
| **2** (X-ray geom.) | | | | | | | | | | |
| B3LYP/6311G(3d)$^f$ | −94.4(−83.4) | −21.1(−10.2) | −33.9(−20.5) | −228.2(−219.5) | 207.1(209.3) | −58.0(−50.4) | −19.9(−10.2) | −64.3(−58.5) | −89.9(−82.7) | 70(75) |
| B3LYP/cc-PVTZ | −79.1 | −4.9 | −18.1 | −214.4 | 209.2 | −43.1 | −2.4 | −46.1 | −80.8 | 78.4 |
| **2** (exp.) | **−85** | **−10** | **−30** | **−200** | **190** | **−56** | **−20** | **−60** | **−95** | **75** |

$^a$ In ppm, at B3LYP/6-311G(3d)//B3LYP/6-31G(d) unless stated otherwise. $^b$ For structures see Figure 4. $^c$ ∠HOSiO = 90°. $^d$ B3LYP/6-311G(3d)// B3LYP/6-311G(d,p). $^e$ Optimized at B3LYP/6-311+G(d,p). $^f$ In parentheses at B3LYP/6-311G(d)//B3LYP/6-31G(d).

***Scheme 3.*** Pyramidality in N-Donor Stabilized Silaformamide **11-O**



$\Sigma\alpha_i = 328°$
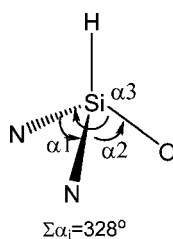
as well as charge distribution and bond orders in model molecules **4-O**−**16-O**.

The discussion below uses the results obtained at B3LYP/ 6-311G(3d); however, the observed trends are the same also at other computational levels (e.g., B3LYP/cc-PVTZ).

**3.2.1.3. Isotropic Chemical Shifts.** As mentioned above, there is a very large upfield shift of as much as 175 ppm in $\delta(^{29}\text{Si}(=\text{O}))_{iso}$ on going from the tricoordinate Si atom in H$_2$Si=O to the four-coordinate Si$^1$(=O) atom in **2** (Table 2). The substituents are responsible for ca. 100 ppm of this total upfield shift. Thus, $\delta(^{29}\text{Si}(=\text{O}))_{iso}$ is shifted upfield from 72.2 ppm in H$_2$Si=O (94 ppm in Me(H)Si=O)) to 25 ppm in methylsilanoic acid **5-O** (due to hydroxy substitution), to 12.6 ppm in silaformamide **6-O** (due to one amino sustituent) and to −7.6 ppm in (H$_2$N)$_2$Si=O (or to −8.5 ppm in cyclic **10-O**) due to two amino substituents. A further upfield shift to −28.9 ppm is observed in silacarbamate **8-O** due to both silyloxy and amino substitution.$^{71}$ When the amino group is rotated by 90° (**9-O**) $\delta(^{29}\text{Si}(=\text{O}))_{iso}$ is shifted back downfield to −8.7 ppm, reflecting the important effect of n(N) → π*(Si=O) conjugation on the chemical shift.$^{72}$ Changing the coordination of the **Si**(=O) atom from three to four, i.e., **14-O** → **13-O**, causes a significant upfield shift of 54 ppm.

**3.2.1.4. Chemical Shift Anisotropy and Chemical Shift Tensors.** The chemical shift anisotropy of the **Si**(=O) atom is represented here by $\Delta\delta = \delta_{11} - \delta_{33}$. $\Delta\delta$ is the largest for the parent H$_2$Si=O silanone (429 ppm), and it decreases in the substituted **7-O**, **8-O** and **14-O** to 313, 327 and 297 ppm, respectively. In tetracoordinate Si(=O) models $\Delta\delta$ decreases further and is in the range 200−290 ppm (Table 2). However, in all model systems and in **2** $\Delta\delta(\text{Si}(=\text{O}))$ is significantly larger than $\Delta\delta$ of the sp$^3$ tetracoordinate **Si**(−O) atom which is in the range 63−117 ppm (Table 2). The large $\Delta\delta(\text{Si}(=\text{O}))$ in **2** and in its model systems may reflect a contribution of double bond character to the Si=O bonds in these compounds.$^{37,39,63-65}$ This point is further discussed below.

The effect of substituents is largest on $\delta_{11}(\text{Si}(=\text{O}))$, it is smaller for $\delta_{33}$, and $\delta_{22}$ is the least affected. For example, on going from H$_2$Si=O to H$_2$NSi(=O)OH (**7-O**) $\delta_{11}$ is shifted upfield from 319 to 114 ppm, $\delta_{22}$ is shifted downfield from 9 to 32 ppm, and $\delta_{33}$ is shifted upfield from −111 to −200 ppm. On changing from a trigonal planar Si(=O) atom to a tetracoordinate pyramidal structure, we find a somewhat similar trend, but in this case also $\delta_{22}$ is shifted upfield. On going from **14-O** to **13-O**, $\delta_{11}$ is shifted significantly upfield from 83 to −7 ppm, respectively. The effect on $\delta_{22}$ and $\delta_{33}$ is smaller (Table 2). To better understand the origin for these large changes we will analyze the direction of the tensor components relative to the

(71) A similar substituent effect is found also in the carbonyl analogues: $\delta(^{13}\text{C}(=\text{O})) = 199$ ppm (acetaldehyde);$^{71a}$ 170.8 ppm (methylacetate);$^{71b}$ 164.9 ppm (formamide);$^{71a}$ 158 ppm (methylcarbamate).$^{71c}$ (a) Stothers, J. B. *Carbon-13 NMR spectroscopy*; Academic Press: 1972. (b) Dorman, D. E.; Bauer, D.; Roberts, J. D. *J. Org. Chem.* **1975**, *40*, 3729–3735. (c) Aldrich Spectral Viewer.

(72) Rotation of the hydroxy group in **5-O** by 90° (∠HOSiO = 90°) causes only a small downfield shift of 7 ppm. The n(O) → π*(Si=O) conjugation is turned off, but in return the conjugation with the second oxygen lone pair comes into effect.
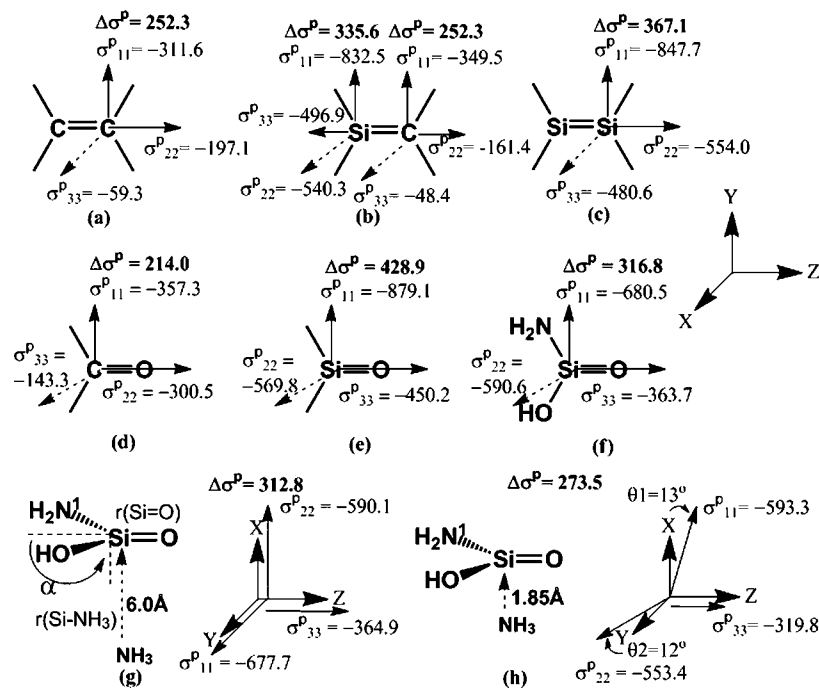
**Figure 5.** Calculated (B3LYP/6-311G(3d)) *paramagnetic* chemical shielding tensor components of doubly bonded compounds. $\Delta\sigma^p = \sigma^p_{33} - \sigma^p_{11}$.

molecular coordinate framework and will evaluate using the NCS method,[55] which MOs affect mostly the paramagnetic contribution ($\sigma^p$) to the chemical shielding tensors.

The total chemical shielding $\sigma$ is a sum of the diamagnetic ($\sigma^d$) and paramagnetic ($\sigma^p$) chemical shielding components. $\sigma^d$ results from the circulation of the electrons induced by the applied magnetic field. The resulting induced local magnetic field opposes the static external magnetic field causing shifts to highfield (shielding). $\sigma^d$ depends on the electron density distribution and inversely on their distance from the nucleus. The effect of substituents and environment on $\sigma^d$ is generally small (and in our case as well, e.g., $\sigma^d$ (Si(=O)) is 882, 884, and 880 ppm in $H_2Si=O$, **7-O**, and the tetracoordinate **15-O**, respectively). The paramagnetic contribution $\sigma^p$ results from paramagnetic electronic currents that are induced by the applied magnetic field via coupling of occupied and virtual orbitals. These induced currents induce a local magnetic field that enhances the applied magnetic field thus causing downfield shifts (deshielding). According to Ramsey's formula,[73,74] $\sigma^p$ is inversely proportional to the energy separation between the mixed orbitals; it is proportional to the degree of overlap of the coupling orbitals and is proportional to the inverse cube of the distance of the shielding electrons from the nucleus in question. The measured (and calculated) chemical shift $\delta$ is the chemical shielding $\sigma$ of the atom in question relative to the chemical shielding of a reference compound, in our case tetramethylsilane (TMS) ($\delta = \sigma_{TMS} - \sigma$). Note that smaller $\sigma$ values mean a *downfield* shift while smaller $\delta$ values mean an *upfield* shift!

The chemical shifts and anisotropy of low-coordinate atoms in unsaturated compounds are mainly determined by the paramagnetic contribution to the chemical shielding, $\sigma^p$.[37,39,63-65] In doubly bonded systems (e.g., olefins, silenes, and disilenes) the most downfield shifted paramagnetic tensor component, $\sigma^p_{11}$,

lies in the molecular plane and perpendicular to the molecular axis (Figure 5, **a**, **b**, **c**). The major contribution to this tensor component is attributed to the mixing of the $\sigma(M=E)$ and $\pi^*(M=E)$ orbitals. In several cases changes in the chemical shifts of these compounds (e.g., caused by substituents) were found to be strongly affected by the changes in the energy separation between these two orbitals.[37,39,63-65] In ethylene and disilene $\sigma^p_{22}$ lies in the molecular plane and is directed along the molecular axis, and $\sigma^p_{33}$ which is shifted to the highest field, lies perpendicular to the molecular plane. It is important to note the large anisotropy between $\sigma^p_{11}$ and $\sigma^p_{33}$. A similar directionality is also found in $H_2C=O$ (Figure 5, **d**). In **d**, according to NCS calculations, the major contribution to $\sigma^p_{11}(^{13}C)$ is associated with the $\sigma(C=O)$ orbital and is attributed to $\sigma(C=O) \rightarrow \pi^*(C=O)$ mixing.[55,75] As in formaldehyde also in $H_2Si=O$ the major contribution to $\sigma^p_{11}$ comes from the $\sigma(Si=O)$ orbital. However, the chemical shift anisotropy ($\Delta\sigma^p = \sigma^p_{11} - \sigma^p_{33}$) is significantly larger in silanone than in formaldehyde (429 ppm vs 214 ppm, respectively), similarly to the trend found for ethylene vs disilene. Upon substitution by both hydroxy and amino substituents the paramagnetic anisotropy decreases significantly to 317 ppm (Figure 5, **f** and Table 2, **7-O**). Both $\sigma^p_{11}$ and $\sigma^p_{33}$ are shifted upfield, but the shift in $\sigma^p_{11}$ is significantly larger. $\sigma^p_{22}$ is hardly affected by these substituents. One of the main reasons for the significant upfield shift of $\sigma_{11}$ in **f** (**7-O**) is the increase in $\Delta E(\pi^*(Si=O)-\sigma(Si=O))$ from 7.5 eV in $H_2Si=O$ to 9.8 eV in **7-O** (B3LYP/6-31G(d)).[76]

To understand the significant changes in the NMR caused by changing the coordination of the **Si**(=O) atom from tricoordinate to tetracoordinate (Table 2), we compare the

(73) Ramsey, N. F. *Phys. Rev.* **1950**, *78*, 699–703.
(74) *Molecular Quantum Mechanics*, 3rd ed.; Atkins, P. W., Friedman, R. S., Eds.; Oxford University Press: Oxford, U.K., 1997.
(75) Kirby, C. W.; Lumsden, M. D.; Wasylishen, R. E. *Can. J. Chem.* **1995**, *73*, 604–613.
(76) Rotation of the amino group in **8-O** by 90° (forming **9-O**) turns off the n(N)−π* conjugation and reduces $\Delta E(\pi^*(Si=O)-\sigma(Si=O))$ from 9.5 eV in **8-O** to 9.2 eV in **9-O** (B3LYP/6-31G(d)), causing a downfield shift of 34 ppm in $\sigma_{11}^p$ (B3LYP/6-311G(3d)).
(77) (a) Reed, A. E.; Weinstock, R. B.; Weinhold, F. *J. Chem. Phys.* **1985**, *83*, 735–746. (b) Wiberg, K. B. *Tetrahedron* **1968**, *24*, 1083–1096.

*paramagnetic* chemical shifts of model structures **g** and **h** (Figure 5). For ease of analysis all geometric parameters are optimized, except for the OSi(=O)N$^1$ plane which is kept planar. The effect of pyramidalization on the NMR shifts is small (see below). In **g**, the attached ammonia group is far (6.0 Å) and the interaction is minor, and the NMR tensor components are very similar to those of **f**. When NH$_3$ approaches to a distance of 1.85 Å (**h**), a dramatic change in the NMR tensor components occurs: the anisotropy decreases from 313 ppm in **g** to 273 ppm in **h**, and $\sigma^p_{11}$ (pointing in the Y direction, i.e., in the molecular plane and perpendicular to the molecular axis) is shifted significantly upfield from −678 ppm in **g** to −553 ppm in **h**, and it is now *at a higher field* than the tensor component which is directed along the X coordinate, i.e., perpendicular to the molecular plane (this tensor component is hardly changed upon complexation with the ammonia group). Consequently, in structure **h**, having a 4-fold coordination, $\sigma^p_{11}$ points in the X direction, perpendicular to the molecular plane while $\sigma^p_{22}$ is in the molecular plane (Figure 5) and perpendicular to the molecular axis, in contrast to the known typical NMR picture in doubly bonded compounds where the most *paramagnetic* tensor component is in the molecular plane and perpendicular to the molecular axis. Furthermore, the large difference between the two tensor components which lie perpendicular to the double bond axis in **a**−**g** (Figure 5) decreases significantly in **h**. For example, $\sigma^p_{33} - \sigma^p_{11} = 367$ ppm in **c**, $\sigma^p_{22} - \sigma^p_{11} = 309$ ppm in **e** and 90 ppm in **f**, while it is 40 ppm in **h** (see also the similarity of $\delta_{11}$ and $\delta_{22}$ in tetracoordinate **12-O**, **13-O**, **2**, and **15-O** vs the large difference between the values of these components in tricoordinate molecules **4-O**−**11-O**, Table 2).

This change in the directionality of the chemical shift tensor components between **h** and the other molecules in Figure 5 may hint to a change in the nature of the Si=O bonding in the tetracoordinate compounds such as **2**. It should however be pointed out that also in **h** the $\sigma$(Si=O) orbital contributes significantly to $\sigma^p_{22}$ (directed in the Y direction), but its contribution is by ca. 200 ppm smaller than that in **g**, leading to its considerable upfield shift. Graphs showing the change in the chemical shift tensor components $\delta_{XX}$, $\delta_{YY}$, and $\delta_{ZZ}$ and $\delta_{11}$, $\delta_{22}$, and $\delta_{33}$ in **g** as a function of $r(\text{Si}\cdots\text{NH}_3)$ are presented in Figure 1S in the Supporting Information, and they demonstrate a similar behavior to that of the paramagnetic shielding components.

We have shown above that the tricoordinate silanones, silanoic silylesters (**4-O**−**10-O**, **14-O**), and the tetracoordinate compounds (**11-O**−**13-O** and **2**) differ by two major geometric parameters, that is, a longer Si=O bond and pyramidality of the Si(=O) center in the latter. However, we have found that the chemical shifts are hardly affected by either changing $r(\text{Si}=\text{O})$ from 1.52 to 1.565 Å or by changing the angle $\alpha$ (for definition see **g**, Figure 5) which reflects the pyramidality at Si from 90° to 65° in both **g**, $r(\text{Si}\cdots\cdots\cdots\text{NH}_3) = 6.0$ Å and **h**′, $r(\text{Si}-\text{NH}_3) = 1.998$ Å (see Figures 3S and 4S in the Supporting Information).

In summary, the significant upfield shift on going from model molecules with a tricoordinate silicon atom (e.g., **8-O**) to molecules with a tetracoordinate silicon atom (**11-O**−**13-O**) results *from the change in the coordination number of the silicon atom and the resulting change in charge distribution (see below), while the geometric changes have no significant effect.* The most significant changes are observed for the chemical shift tensor component pointing in the Y direction, i.e., in the R$_2$Si=O plane and perpendicular to the Si=O axis.

***Table 3.*** Calculated (B3LYP/6-31G(d)) Natural Population Analysis (NPA) Charges and Wiberg Bond Indices (WBI) in Compounds with a Si=O Bond, in Their Si=S Analogues and in the Experimental **2** and **3**$^a$

| | Si=O | | | | Si=S | | | |
|---|---|---|---|---|---|---|---|---|
| Compound | *q*(Si) | *q*(O) | Δ*q* | WBI$^b$ | *q*(Si) | *q*(S) | Δ*q* | WBI |
| **4-O, 4-S** | 1.47 | −1.00 | 2.47 | 1.5 | 0.93 | −0.56 | 1.49 | 1.9 |
| **5-O, 5-S** | 2.05 | −1.07 | 3.12 | 1.4 (0.7) | 1.64 | −0.70 | 2.34 | 1.8 |
| **7-O, 7-S** | 2.14 | −1.09 | 3.23 | 1.4 (0.7) | 1.75 | −0.74 | 2.48 | 1.7 |
| **8-O, 8-S** | 2.17 | −1.08 | 3.26 | 1.4 (0.6) | 1.78 | −0.72 | 2.5 | 1.7 |
| **9-O, 9-S** | 2.16 | −1.07 | 3.23 | 1.4 (0.7) | 1.77 | −0.69 | 2.47 | 1.7 |
| **10-O, 10-S** | 2.08 | −1.09 | 3.16 | 1.4 | 1.60$^c$ | −0.67$^c$ | 2.27$^c$ | 1.7$^c$ |
| **11-O, 11-S** | 1.86 | −1.15 | 3.01 | 1.3 | 1.35$^c$ | −0.76$^c$ | 2.11$^c$ | 1.5$^c$ |
| **12-O, 12-S** | 2.27 | −1.19 | 3.46 | 1.2 | 1.82$^c$ | −0.82$^c$ | 2.63$^c$ | 1.5$^{c,d}$ |
| **13-O, 13-S** | 2.29 | −1.20 | 3.49 | 1.2$^e$ | 1.90 | −0.84 | 2.75 | 1.5 |
| **14-O, 14-S** | 2.20 | −1.11 | 3.31 | 1.3 (0.7) | 1.80 | −0.74 | 2.54 | 1.7 |
| **15-O, 15-S** | 2.22 | −1.18 | 3.40 | 1.3 | 1.84 | −0.85 | 2.69 | 1.5 |
| **16-O, 16-S** | 2.22 | −1.25 | 3.46 | 1.1 | 1.82 | −0.99 | 2.80 | 1.3 |
| **2**$^f$, **3**$^f$ | 2.32 | −1.22 | 3.54 | 1.1 | 1.90 | −0.83 | 2.73 | 1.50 |

$^a$ For the numbering and structures of the compounds see Figure 4 (Si=O) and Figure 1S of the *Supporting Information* (Si=S). $^b$ In parentheses the Si−O WBI. $^c$ At B3LYP/6-311G(d,p). $^d$ WBI of Si(=S)−O bond is 0.56 and that of H$_3$Si−O is 0.62. $^e$ WBI of the exocyclic C=C bond is 1.71. $^f$ Optimized geometry (B3LYP/6-31G(d)).

***Scheme 4.*** Resonance Forms of H$_2$Si=O
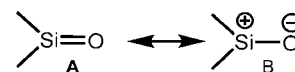


Interestingly, the isotropic chemical shift, the anisotropy, as well as $\delta_{11}$, $\delta_{22}$, and $\delta_{33}$ in **2** are similar to those in the anionic model **16-O**. Also, $r(\text{Si}=\text{O})$ in **2** (optimized geometry) and $r(\text{Si}-\text{O}^-)$ in anion **16-O** are significantly longer than $r(\text{Si}=\text{O})$ in tricoordinate model systems **4-O**−**10-O**. These trends point to a greater degree of zwitterionic character (Si$^+$−O$^-$) in silanoic silylester **2** than in a tricoordinate Si=O double bond. This conclusion is supported by the calculated Natural Population Analysis (NPA)$^{77a}$ charges and Wiberg Bond Indices (WBI)$^{77b}$ that were calculated for the model molecules and for **2** (Table 3) and are discussed below.

**3.2.1.5. Bond Polarities and Bond Orders.** NBO analysis shows that the Si=O bond in H$_2$Si=O has two bonding orbitals, a $\sigma$-orbital with an sp$^{1.7}$ hybridized Si and a $\pi$-orbital. Both orbitals are very strongly polarized toward the oxygen atom (i.e., 80% of the NBO density resides on the oxygen atom), pointing to a high contribution from the zwitterionic resonance structure (B, Scheme 4). In a previous study Guselnikov and co-workers concluded, based on ELF and AIM analyses that the electronic structure of H$_2$Si=O is dominantly zwitterionic having a $\sigma$(Si$^+$−O$^-$) bond with three lone pairs in the valence shell of the oxygen.$^{78}$

The calculated NPA charges show that in all model molecules the Si=O bonds are highly polarized with charges on the oxygen in the range −1.0 to −1.2 el. The Si=O bond polarity increases significantly upon changing the Si coordination number from 3 to 4; for example, the NPA charge on Si in **8-O** is 2.17 el., and it increases to 2.32 el. in **2** (Δ*q* = 3.26, 3.46, and 3.54 el. in **8-O**, **12-O**, and **2**, respectively). This can be explained by the coordination of an additional electronegative amino group to the Si atom, which helps to stabilize a higher positive charge on the silicon atom. The change in bond polarity on going from tri- to the tetracoordinae Si center is nicely reflected in the

(78) Avakyan, V. G.; Sidorkin, V. F.; Belogolova, E. F.; Guselnikov, S. L.; Gusel'nikov, L. E. *Organometallics* **2006**, *25*, 6007–6013.
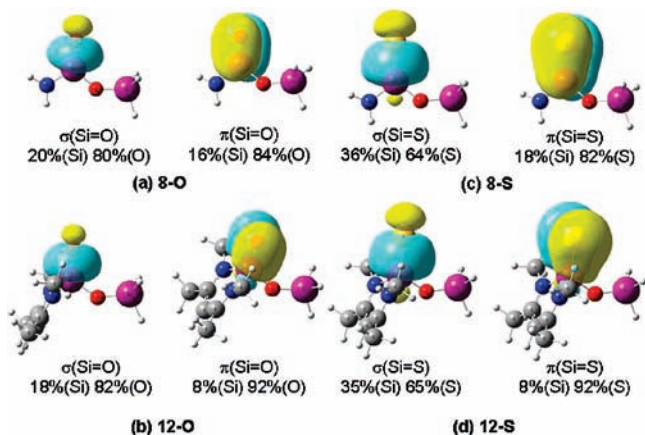
**Figure 6.** Calculated (B3LYP/6-31G(d)) Si=X π- and σ-NBOs in **8-X** and **12-X** (X = O, S) (the percentage is the square of the orbital coefficient on each of the atoms).

polarity of the σ and π Si=X (X = O and S) NBO orbitals (Figure 6). Figure 6 shows that in both **8-O** and **8-S** 82−84% of Si=X π-orbital density is located on X. This high polarity increases even further in the tetracoordinate **12-O** and **12-S** where 92% of the π-NBO resides on O or S, respectively, and only 8% resides on the Si. The polarity of the σ-NBO in **8-O** vs **12-O** and **8-S** vs **12-S** remains unchanged. The conclusion is that the additional coordination affects mainly the polarity of the π-orbital. Another interesting conclusion from the NBO analysis is that while the polarity of the π-orbital in **8-O** and **8-S** (and of **12-O** and **12-S**) is similar, the polarity of the σ-orbital of the thio-compounds is significantly smaller than that of the oxy-compounds (i.e., 65% vs 82% of the σ-NBO densitiy resides on the S and O atoms in **12-O** and **12-S**, respectively, Figure 6) reflecting the smaller electronegativity of S vs O and the overall smaller polarity of the thio-compounds. (Table 3).

Consequently with the increase in bond polarity, the covalent Wiberg bond orders of the Si=X bonds decrease on going from the tricoordinate silicon atoms (WBI = 1.4−1.5 for Si=O and 1.9−1.7 for Si=S)) to tetracoordinate silicon atoms (WBI = 1.1 in **2** and 1.5 in **3**). Nevertheless, WBI(Si=O) in **2** is much higher than that for Si−O single bonds; e.g., WBI(Si−O) of the siloxy group of **2** is only 0.6. In conclusion, the calculations clearly show that the Si=O bond in silanoic silylester **2** is highly polarized pointing to a predominantly zwitterionic Si=O bond with a contribution of some Si=O π-bonding. This conclusion is consistent with the conclusions drawn from experimental and calculated ^{29}Si solid-state NMR measurements.

**3.2.2. Stuctures and NMR Analysis and Bond Properties of Silanoic Thioester 3 and of Model Molecules Containing Si=S Bonds.** Figure 7 shows the calculated bond lengths in silanoic thioester **3** in comparison with its X-ray structure.[30] In addition we also carried out calculations for 12 model molecules containing Si=S double bonds which are analogues of the Si=O molecules discussed above (for a full list of all Si=S model molecules and their schematic structures, see Figure 1S of the Supporting Information). For **3** there is good agreement between the calculated and measured Si=S bond length, while the calculated Si−N and Si−O bond lengths are by 0.03−0.04 Å longer than the experimental ones.

The calculated values of [29]Si(=S) and [29]Si(−O) isotropic chemical shift values of thio- model molecules and of the silanoic thioester **3** are given in Table 4.
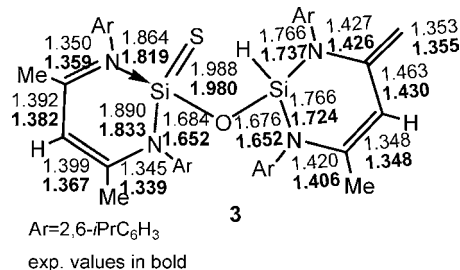


**Figure 7.** Optimized (B3LYP/6-31G(d)) and X-ray (in bold) bond lengths (Å) of silanoic thioester **3**.

Table 4 shows that the calculated (B3LYP/cc-PVTZ) δ([29]Si(=S))$_{iso}$ (using either the X-ray structure of **3** or the optimized structure) are in very good agreement with the experimental NMR data with a deviation of only 1−2 ppm. However, a comparison of the individual tensor components shows larger deviations of ca. ± (20−30) ppm for δ$_{11}$ and δ$_{22}$ and of ca. 5−3 ppm in δ$_{33}$.

A comparison of the structural (Figure 1S, Supporting Information) and NMR data (Table 4) for the thio-compounds with that in Figure 4 and Table 2 for the oxy-compounds shows that the trends in the effects of substituents and the effect of the change in the coordination of the Si=X subunit (X = O, S) both on structures and on the NMR chemical shifts are similar in Si=S and Si=O compounds. However there are two major differences between these two groups of compounds. In the experimental (and calculated) data of **3**, as well as in all tri- and tetracoordinate Si=S model compounds, there is a significant downfield shift of δ([29]Si(=S))$_{iso}$ in comparison to the corresponding δ([29]Si(=O))$_{iso}$; e.g., in **3** and **2** the measured δ([29]Si(=S))$_{iso}$ and δ([29]Si(=O))$_{iso}$ are −38.7 and −85.0 ppm, respectively. The downfield shift in the thio-compounds is most dominant in δ$_{11}$, e.g., 87 ppm in **3** compared to −10 ppm in **2**, and is much smaller in δ$_{22}$ and δ$_{33}$. These significant changes can be attributed to the smaller ΔE(σ−π*) in the thio com-pounds; e.g., it is 8.9 eV in H$_2$NSi(=S)OH and 9.9 eV in H$_2$NSi(=O)OH, which according to Ramsey's formula[73,74] leads to a larger paramagnetic contribution to δ$_{11}$ and consequently to a downfield shift in the thio-acid. The significant large downfield shift in δ$_{11}$ of the thio-compounds and the negligible difference in δ$_{33}$ (e.g., −215 ppm in **3** and −200 ppm in **2**) leads to a significantly larger Δδ in the thio-compounds, e.g., 302 ppm in **3** vs 190 ppm in **2** (measured) and 393 ppm vs 313 ppm (calculated) in H$_2$NSi(=S)OH (**7-S**) and in H$_2$NSi(=O)OH (**7-O**). Similarly to the Si=O compounds also for the Si=S compounds Δδ is significantly larger in the tricoordinate than in the four-coordinate compounds. A similar trend is found also for C=O and C=S compounds. For example, in acetamide and thioacetamide the measured δ(^{13}C)$_{iso}$ is 177 and 330 ppm, respectively; δ$_{11}$ is 243 and 330 ppm, respectively; and Δδ is 157 and 269 ppm, respectively.[75]

As expected from the smaller electronegativity of the sulfur atom, the calculated NPA charges for the Si=S bond in **3** and in all model molecules show that the Si=S bonds are signifi-cantly less polarized than the Si=O bonds (Table 3). For example, the NPA charge on Si in the Si=S bond in **3** (optimized geometry) is only 1.9 compared to 2.3 in the corresponding Si=O bond of **2**. Consequently, the covalent bond order of the Si=S bond in **3** is significantly larger (WBI = 1.5) than that of the corresponding Si=O bond (WBI = 1.1) in **2**. Thus, in the Si=S compounds the zwitterionic form (Si[+]−S[−]) plays a smaller role than in the Si=O compounds and the

***Table 4.*** Calculated $^{29}$Si NMR Chemical Shifts[a] of Compounds with a Si=S Bond

| compound[b] | Si=S | | | | | Si−O | | | | |
|---|---|---|---|---|---|---|---|---|---|---|
| | $\delta_{iso}$ | $\delta_{11}$ | $\delta_{22}$ | $\delta_{33}$ | $\Delta\delta$ | $\delta_{iso}$ | $\delta_{11}$ | $\delta_{22}$ | $\delta_{33}$ | $\Delta\delta$ |
| **4-S** | 157.7 | 530.2 | 11.5 | −68.6 | 598.8 | − | − | − | − | − |
| **5-S** | 122.5 | 383.7 | 120.6 | −136.9 | 520.6 | − | − | − | − | − |
| **7-S**[c] | 49.7 | 226.8 | 88.3 | −166.1 | 392.9 | − | − | − | − | − |
| **8-S** | | | | | | | | | | |
| B3LYP/6-311G(3d) | 37.1 | 219.4 | 80.2 | −188.8 | 408.3 | −43.4 | −6.8 | −9.9 | −113.6 | 106.8 |
| MP2/6-311G(3d) | 43.4 | 210.2 | 90.0 | −170.1 | 380.3 | −40.5 | −1.9 | −3.6 | −116.0 | 114.1 |
| B3LYP/cc-PVTZ | 48.5 | 229.2 | 83.0 | −166.7 | 395.9 | −36.0 | 4.3 | −0.7 | −109.8 | 114.1 |
| MP2/cc-PVTZ | 45.6 | 206.6 | 86.9 | −156.9 | 363.2 | −36.9 | −1.9 | −4.5 | −104.2 | 110.4 |
| CCSD/cc-PVTZ | 50.3 | 216.8 | 90.4 | −156.2 | 373 | −33.8 | −1.3 | −3.4 | −96.7 | 95.4 |
| **9-S** | 66.3 | 288.3 | 94.3 | −183.6 | 471.9 | −43.1 | −6.6 | −10.4 | −112.3 | 105.7 |
| **10-S**[d] | 56.4 | 267.3 | 88.6 | −186.7 | 454.0 | − | − | − | − | − |
| **11-S**[d] | −25.5 | 117.4 | 21.3 | −215.2 | 332.6 | − | − | − | − | − |
| **12-S**[d] | | | | | | | | | | |
| B3LYP/6-311G(3d) | −32.3 | 74.9 | 51.4 | −223.2 | 298.1 | −54.9 | −14.6 | −21.7 | −128.6 | 114.0 |
| B3LYP/cc-PVTZ | −21.4 | 63.9 | 59.9 | −206.1 | 270.0 | −43.7 | 1.8 | −8.9 | −124.1 | 125.9 |
| **13-S** | −36.6 | 74.2 | 52.5 | −236.4 | 310.6 | −64.3 | −29.1 | −79.7 | −84.0 | 55.0 |
| **14-S** | 24.8 | 190.1 | 77.3 | −192.2 | 382.3 | −61.4 | −21.9 | −69.3 | −92.9 | 71.0 |
| **15-S** | −17.1 | 90.2 | 59.6 | −201.2 | 291.2 | −51.3 | −12.9 | −17.2 | −123.9 | 111 |
| **16-S**[e] | −13.4 | 53.0 | 21.3 | −114.6 | 167.6 | −70.5 | −23.6 | −30.8 | −157.0 | 86.5 |
| **3** (opt. geom.) | | | | | | | | | | |
| B3LYP/6-311G(3d) | −47.2 | 52.9 | 40.5 | −235.1 | 288.0 | −62.9 | −22.5 | −73.5 | −92.8 | 70.3 |
| B3LYP/cc-PVTZ | −36.7 | 61.2 | 47.1 | −218.5 | 279.7 | −50.2 | −9.3 | −58.7 | −82.4 | 73.1 |
| **3** (X-ray geom.) | | | | | | | | | | |
| B3LYP/6-311G(d) | −38.7 | 58.7 | 39.4 | −214.3 | 273.0 | −57.8 | −13.6 | −72.8 | −86.9 | 73.3 |
| B3LYP/cc-PVTZ | −39.8 | 55.2 | 35.4 | −210.2 | 265.4 | −53 | −6.4 | −65.9 | −86.5 | 80.1 |
| **3 exp.** | **−38.7** | **87** | **11** | **−215** | **302** | **−53.5** | **−3** | **−54** | **−104** | **101** |

 *[a]* In ppms, at B3LYP/6-311G(3d)//B3LYP/6-31G(d) unless stated otherwise. *[b]* The compounds and numbering are analogous to to those in Figure 4. For optimized bond lengths see Figure 1S of the Supporting Information. *[c]* Chemical shift values at MP2/6-311G(3d) as well as at B3LYP, MP2 and CCSD with cc-PVTZ basis set are provided in Table 2S of the Supporting Information. *[d]* B3LYP/6-311G(3d)//B3LYP/6-311G(d,p). *[e]* B3LYP/6-311G(3d)//B3LYP/6-311+G(d,p).

double-bond contribution to the Si=S bond is higher. This conclusion is consistent with the findings of Guselnikov and co-workers that the Si=S bond in $H_2Si=S$ has a double bond character while the Si=O bond in $H_2Si=O$ has a zwitterionic character with three lone pairs on the oxygen atom.[78] This is also reflected in the fact that the chemical shift values calculated for the anionic model molecule **16-S** show a larger deviation from the experimental NMR results for **3** than in the analogous Si−O systems (**16-O** vs **2**) and is also reflected in the larger $\Delta\delta$ value in **3** relative to **16-S**. However, despite these differences, the data show that the Si=S bond polarity increases significantly upon changing the Si coordination number from 3 to 4, and the covalent bond orders decrease similarly to the trends found for the Si=O bonds.

## 4. Conclusions

This paper describes $^{29}$Si solid state NMR measurements of silylene **1**, silanoic silylester **2**, and silanoic thioester **3** as well as the results of detailed DFT and *ab initio* calculations which were carried out for **2** and **3** and for smaller model compounds with Si=X (X = O, S) bonds. In general there is good agreement between calculations and experiment which give support to the chemical shift assignment deduced from experiment.

The solid-state $^{29}$Si NMR of the stable silylene **1** revealed a highly anisotropic chemical shift tensor comparable to that in other N-heterocyclic silylenes.

The experimental and computational study of **2** and **3** combined with the computational study of smaller model molecules provides a deeper understanding of the isotropic and tensor components of their NMR chemical shifts. The calculations reveal that in **2** $\delta(^{29}Si(=O))_{iso}$ is shifted upfield relative to $H_2Si=O$ by as much as 175 ppm; substituents are responsible

for ca. 100 ppm of this shift, while the remaining upfield shift is caused by the change in the coordination number at the Si=O moiety from three to four due to the coordination with an additional amino ligand. The chemical shift values are practically not affected by the Si=X bond length or the degree of pyramidality at the Si=X center caused by the increase in coordination number.

The change in the silicon coordination from three to four affects mostly the tensor component which lies in the molecular plane and is perpendicular to the molecular axis ($\delta_{YY}$) but it hardly affects the tensor component which is perpendicular to the molecular plane ($\delta_{XX}$), leading to a nearly cylindrical symmetry in the tensor components that lie in the *XY* plane. This contrasts with the large anisotropy found in this plane in typical doubly bonded compounds (Figure 7).

$\delta(^{29}Si(=S))_{iso}$ in **3** is shifted downfield significantly relative to that in **2** (a similar trend is found in the smaller model Si=S vs Si=O molecules). This downfield shift can be explained by the smaller $\sigma-\pi^*$ energy difference in the Si=S bond.

The NMR measurements and calculations of the tensor components, bond polarities, and Wiberg bond indices of **2** and **3** having a *four-coordinate* silicon−chalcogen double bond reveal that the Si=O moiety in **2** has a high contribution from a zwitterionic $Si^+-O^-$ structure, yet the bond has a significant contribution of a Si=O $\pi$-bonding. The Si=S bond in the thioester **3** shows a larger Si=S double bonding character and a smaller zwitterionic contribution. In conclusion, in both **2** and **3** the *tetracoordinate* Si=X subunit exhibits a pronounced double bond character, which is more significant in **3**.

**Note Added after ASAP Publication.** Labels were added to Scheme 1 and structures were corrected in Figure 5g,h in the version of this article published April 14, 2010.

**Supporting Information Available:** Optimized structures of silanoic thioester and model systems containing Si=S bonds (Figure 1S); Calculated isotropic and tensor components of the chemical shifts as a function of $r(Si-NH_3)$, the pyramidality at the Si=O center, and $r(Si=O)$ (Figures 2S−4S); Calculated isotropic chemical shielding of TMS (Table 1S); Calculated $^{29}Si$ NMR chemical shifts of **7-O** and **7-S** at B3LYP, MP2, and CCSD with 6-311G(3d) and cc-PVTZ basis sets (Table 2S). Cartesian coordinates and total energies (hartrees) of **2** and **3** and other smaller model compounds (Table 3S); Complete ref 56. This material is available free of charge via the Internet at http://pubs.acs.org.

JA1004812